First Observation of ECH by Electron Bernstein Waves Excited via X-B Mode Conversion Process in LHD

Hiroe IGAMI, Takashi SHIMOZUMA, Shin KUBO, Kazunobu NAGASAKI[1)], Shigeru INAGAKI, Yasuo YOSHIMURA, Takashi NOTAKE, Kunizo OHKUBO, Takashi MUTOH and LHD experimental group

National Institute for Fusion Science, Toki 509-5292, Japan
[1)]*Institute of Advanced Energy, Kyoto University, Uji 611-0011, Japan*

(Received 1 August 2006 / Accepted 20 September 2006)

In a magnetic field configuration of the Large Helical Device (LHD), when the extraordinary mode (X-mode) waves are obliquely injected from a bottom antenna, it can directly access the upper hybrid resonance (UHR) layer from the high field side and excite electron Bernstein waves (EBWs) without the need for any additional reflecting mirror antenna. A localized power absorption is observed in the low field side of the electron cyclotron resonance (ECR) layer. This result suggests electron cyclotron heating (ECH) by mode converted EBWs excited via X-B mode conversion process.

Keywords: electron cyclotron heating, electron Bernstein wave, power modulation, FFT analysis

DOI: 10.1585/pfr.1.052

Electron cyclotron heating (ECH) and current drive (ECCD) by using electron Bernstein waves (EBWs) are promising ways of ECH/ECCD in high density plasma core or low temperature peripheral region instead of using the normal electromagnetic ordinary (O-) or the extraordinary (X-) mode. Thus, ECH/ECCD by using EBWs have been studied also in regard to the helical configuration [1]. One way to excite EBWs is to inject the X-mode waves from the high field side of the upper hybrid resonance (UHR) layer [2]. For local heating, it is more effective to inject the X-mode waves so that they can access the UHR layer directly without suffering multi-reflections. Therefore, this method sometimes requires the installation of an additional reflecting mirror antenna close to the plasma surface [2].

Figure 1 shows the cross sections of the plasma and incident microwave beam in vacuum for a magnetic configuration (R_{axis} = 3.55 m, B_{axis} = 2.789 T) of the Large Helical Device (LHD), where R_{axis} is the distance from the center of the torus to the magnetic axis and B_{axis} is the magnetic field strength at the magnetic axis. In beam injection case (a) or (b) as shown in Fig. 1, the incident beam approaches the fundamental electron cyclotron resonance (ECR) layer from the high-field side. If the beam passes through the ECR layer without absorption, it can access the UHR layer and then excite EBWs without encountering any cutoff. Thus we call the region surrounded by the ECR layer and vacuum vessel wall the "XB access window". This experimental configuration does not require any additional reflecting mirror antenna close to the plasma surface

A microwave beam of 84 GHz, 235 kW was injected with 34 Hz, 100% power modulation to the plasma sustained by the neutral beam injection (NBI). Figure 2 shows a typical set of discharge waveforms seen in the experiment. Perturbations of the ECE signals related to the electron temperature T_e and the stored energy W_p are observed

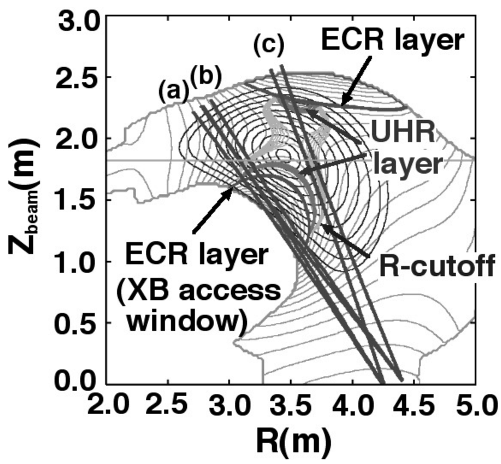

Fig. 1 Cross sections of the plasma and incident microwave beam in vacuum for a magnetic configuration (R_{axis} = 3.55 m, B_{axis} = 2.789 T). R is the direction of the major radius. Z_{beam} is the direction on the plane where the incident microwave beam passes. The mod-B surface, the magnetic flux surface (normalized minor radius ρ), the positions of the ECR layer, the UHR layer and the R-cutoff are represented in contour.

author's e-mail: igami@LHD.nifs.ac.jp

coincidentally with the ECH pulse. In Fig. 3, profiles of the 34 Hz perturbation amplitude and the phase of ECE signals are plotted versus the normalized minor radius ρ for each beam injection case (a), (b), and (c) shown in Fig. 1. These profiles are obtained by Fast Fourier Transform (FFT) analysis. Because the modulation frequency is about $(3 \sim 4)/\tau_E$, where τ_E is the energy confinement time, the absorption effect is dominant compared to the effect of thermal transport in the perturbation amplitude and phase near the absorption region. Thus the region where the perturbation amplitude peak and the perturbation phase bottom coincide indicates the power absorption region. In the case (a), when the X-mode waves are injected, a narrow amplitude peak appears in the lower-field/ρ side of the ECR layer ($\rho \sim 0.47$), although the incident beam approaches from the higher-field/ρ side. The phase bottom is located around the green amplitude peak. In contrast when the O-mode waves are injected, the amplitude peak and the phase bottom are in the higher-field/ρ side ($\rho \sim 0.7$). In case (b), in both cases of X- and O-mode injection, the peaks of the amplitude profiles are located in the higher field/ρ side of the ECR layer. The phase bottom are also at the peaks. In case (c), the perturbation amplitude peak can be seen near $\rho = 0.7$ in the X-mode injection case and $\rho = 0.5$ in the O-mode injection case. However, the phase bottom do not coincide the amplitude peaks in both cases. The absorbed power can be roughly estimated from the perturbation amplitude profile and electron density profile reconstructed by Abel inversion.

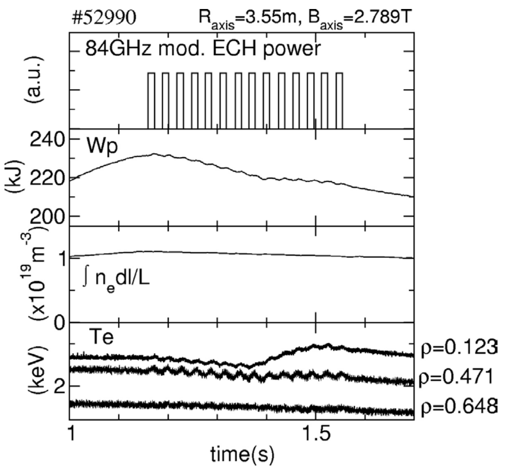

Fig. 2 Typical set of the discharge waveforms in beam injection case (a) shown in Fig. 1. From the top row, ECH pulse, stored energy (W_p), line averaged density ($\int n_e dl/L$), and ECE signals (T_e) at ρ = 0.123, 0.471, 0.648 are shown.

We injected the beam in a manner very similar to that of case (a) shown in Fig. 1 though slightly closer to the vacuum vessel wall. In this injection case, we changed the X-mode purity shot by shot. The amplitude and phase profiles are similar to those in case (a) for the cases of X- and O-mode injection. As shown in Fig. 4 (I), as the X-mode purity increases, the sum of the absorbed power in the inner region ($\rho < 0.6$) increases and the sum in the outer region decreases. We also change the X-mode purity for case (b). As shown in Fig. 4 (II), the sum in the inner region remains almost the same and the sum in the outer region changes with increases in the X-mode purity.

When the incident waves have a certain level of parallel refractive index, the absorption of the X-mode waves is strong even for the fundamental resonance frequency. The result of ray tracing shows that complete X-mode power absorption occurs at the high-field side of the ECR layer where $\rho \sim 0.75$ in the case (a) and $\rho \sim 0.66$ in the case (b). Note that the ray is refracted to the high density region (low ρ side) compared to the vacuum beam. For the power absorption region, the latter agrees with the experimental result though the former does not. Different mechanisms of heating may exist in case (a) when X-mode waves are injected. The actual absorption of the X-mode waves is weaker than the calculation result for some reason

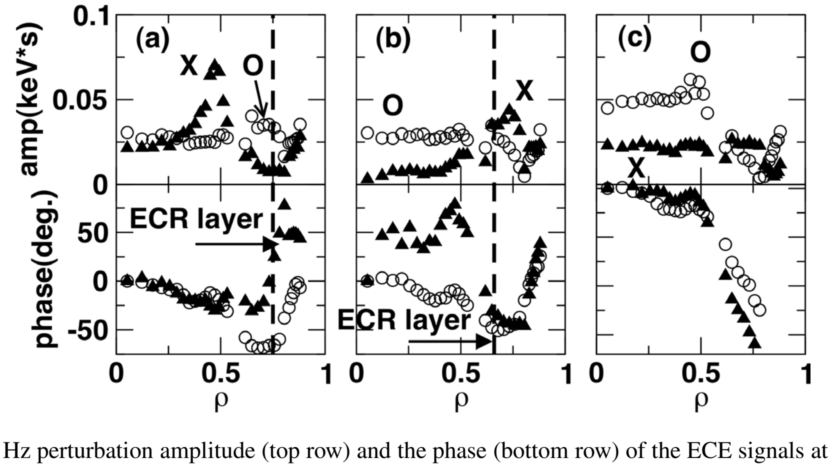

Fig. 3 Profiles of the 34 Hz perturbation amplitude (top row) and the phase (bottom row) of the ECE signals at each channel represented by ρ for each case of X-mode (triangles) and O-mode (circles) injection. Each column marked with (a), (b), and (c) corresponds to the beam injection cases (a), (b), and (c) shown in Fig. 1. The positions of the ECR layer which the refracted X-mode waves encounter are also represented in the columns (a) and (b).

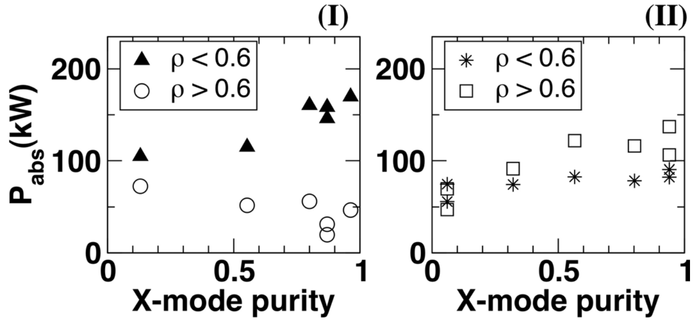

Fig. 4 Sum of the absorbed power in the inner region ($\rho < 0.6$) and the outer region ($\rho > 0.6$). (I): Beam injection case similar to case (a) as shown in Fig. 1. (II): Beam injection case (b) as shown in Fig. 1.

and a part of the wave power can access the UHR layer. ECH by mode converted EBW can occur in this case. In case (c), the incident X-mode waves meet the right handed cyclotron cutoff (R-cutoff) and are reflected toward various directions. The reflected waves are absorbed in the plasma after multi reflection. When the O-mode waves are injected, it passes through the plasma and is reflected at the vacuum vessel wall in various directions. The reflected waves are also absorbed after multi-reflection. Therefore, we cannot see clear relationships between the phase bottom and amplitude profiles in case (c).

[1] K. Nagasaki and N. Yanagi, Plasma Phys. Control. Fusion **44**, 409 (2002).
[2] T. Maekawa *et al.*, Phys. Rev. Lett. **86**, 3783 (2001).